energies

MDPI

Article

Experimental Study on Damage Fracture Law of Coal from Solid-Propellant Blasting

Huaibao Chu [1,2], Mengfei Yu [1,*], Bo Sun [1,3,*], Shaoyang Yan [1], Haixia Wei [1], Guangran Zhang [1], Donghui Wang [1] and Jie Xu [1]

[1] School of Civil Engineering, Henan Polytechnic University, Jiaozuo 454000, China
[2] Henan Key Laboratory Underground Engineering and Disaster Prevention, Jiaozuo 454000, China
[3] School of Civil Engineering, Xinyu University, Xinyu 338000, China
* Correspondence: ymf19980922@163.com (M.Y.); bosun0419@163.com (B.S.); Tel.: +86-188-3965-6466 (M.Y.); +86-157-0790-6611 (B.S.)

Abstract: The low permeability of coal seams has always been the main bottleneck restricting coalbed methane drainage. In this paper, a coal seam anti-reflection technology with solid-propellant blasting was proposed, and the composition and proportion of the solid propellants were determined based on the principle of oxygen balance. The authors designed a solid-propellant blasting damage fracture experiment of simulation coal, tested the impact pressure on a blast hole wall, measured the ultrasonic wave velocity, explosive strain and crack propagation velocity, and then revealed the blasting damage fracture process and mechanism of coal based on the experimental results and damage fracture mechanics theory. The history curve of impact pressure time can be divided into three processes including the slow pressurization process, dramatic increase process, and nonlinear pressure relief process. The pressure distribution along the whole blasting hole was uneven, and the peak pressure was relatively small, but the pressure action time was long. The damage and fracture process of coal solid-propellant blasting can be divided into two stages including the rapid damage fracture development stage and the stable slow damage fracture development stage. Firstly, the explosion stress wave produced and rapidly accelerated the radial cracks extension; secondly, the cracks slowly expanded over a large area by the combined effects of the high-pressure gases, the gas, and the original rock stress.

Keywords: coal; solid propellant blasting; borehole wall pressure; damage fracture law; experimental study

Citation: Chu, H.; Yu, M.; Sun, B.; Yan, S.; Wei, H.; Zhang, G.; Wang, D.; Xu, J. Experimental Study on Damage Fracture Law of Coal from Solid-Propellant Blasting. *Energies* **2022**, *15*, 8104. https://doi.org/10.3390/en15218104

Academic Editors: Shengrong Xie and Dongdong Chen

Received: 22 September 2022
Accepted: 26 October 2022
Published: 31 October 2022

1. Introduction

China's energy situation of 'rich coal, less oil, and natural gas' and the stage of economic and social development determine the main energy status of coal, and it will continue to play a supporting role in energy supply for a longer period in the future [1]. At the same time, the energy strategic direction of 'Reducing Coal, Stabilizing Oil and Increasing Gas, Developing New Energy' was proposed by the Chinese government in the 'Energy Development Strategic Plan for 2020–2050'. The proportion of natural gas in energy consumption will increase to about 15% in 2050. The 'increasing reserves and production' of coal-measure gas is one of the important ways to make up for the gap in the natural gas supply. Large-scale firedamp extraction and utilization is an important part of the coal-measure gas industry. Therefore, the effective development and utilization of coal-measure gas resources is an important way to ensure the safety of the national natural gas supply, help the safe production of coal, and achieve the goal of 'peak carbon emissions by 2030 and reach carbon neutrality by 2060' in China.

The reserve of only coalbed methane is about 36.8 trillion m^3 (shallow coalbed methane buried depth of 2000 m) in China, ranking third in the world, and the recoverable quantity

of coalbed methane is about 10 trillion m^3. However, the occurrence conditions of coalbed methane resources in China are complex, the technical requirements are high, the regional adaptability is poor, and the proportions of high-stress tectonic coal and low permeability coal-measure gas resources are high [2,3]. The low permeability of coal seams has become the key to restricting coalbed methane extraction in China. Therefore, it is one of the major scientific and technological needs to promote the construction of a large coal-measure gas industry to develop and improve the key technology of high-efficiency and low-cost coalbed methane extraction, improve the fracture development level of coalbed methane reservoirs, dredge the seepage channel, and improve the permeability of coal reservoirs and achieve the efficient extraction of coalbed methane.

Researchers at domestic and foreign levels have carried out multi-path research to enhance the permeability of coal seams with low permeability and high-gas content and have achieved fruitful research results. The anti-reflection measure of interlayer pressure relief seam making is adopted for low permeability and high gas coal seams with protective layer mining conditions, having good anti-reflection effects, and is a mature technology [4,5]. For most high-gas and low-permeability coal seams without protective layer mining conditions, hydraulic anti-reflection technologies including hydraulic fracturing, hydraulic punching, and hydraulic slotting are the main measures for anti-reflection transformation of low-permeability coal seams [6–9]. However, hydraulic measures require a lot of water resources, and the invasion and retention of water will also cause water lock and water sensitivity damage to the coal reservoir [10]. At the same time, a large amount of water-based fracturing fluid occupies the gas flow channel, thus affecting gas production. In addition, the penetration of hydraulic fracturing fluid containing chemical additives into the surface and underground drinking water layer will also produce a certain degree of pollution [11]. Therefore, researchers in various countries are also actively seeking alternative methods for hydraulic anti-reflection measures. The non-hydration anti-reflection technologies including deep-hole presplit blasting fracturing technology [12], high-energy and high-pressure gas impact [13,14], controllable shock wave impact [15,16], acoustic shock and ultrasonic disturbance [17,18], and liquid nitrogen injection fracturing technology [19] have been widely used. Among them, the fracturing technology with high-energy and high-pressure gas is considered to be a fracturing anti-reflection technology that can be comparable to hydraulic fracturing.

High-energy, high-pressure gas fracturing refers to the use of rapid discharge of high-energy, high-pressure gas impact on the borehole wall to achieve the purpose of fracturing and increasing permeability. Aerospace solid propellants can be treated as weak explosives, they can be excited to produce a large number of high-energy, high-pressure gas products [20]. Therefore, it is feasible to use solid propellants to fracture and increase the permeability of the coal body. Studies have shown that propellant blasting technology can easily fracture coal seams and create multiple cracks that are not controlled by ground stress due to the advantages of the pressure strength and pressure transfer rate [21]. It also generates oscillating high-pressure pulses to enlarge the fracture extension, and it does not require large equipment and is highly adaptable to the environment [22]. At present, solid propellants have been widely used in the field of conventional oil and gas extraction in highly brittle rock formations [23], but its application in the field of coal reservoir permeability enhancement is still in the initial stage, especially the damage fracture mechanism of the coal body from solid-propellant blasting is still unclear.

Aiming at the characteristics of high gas and low permeability of coal reservoirs in China, this paper proposes a solid-propellant blasting, permeability-increasing technology. Firstly, the composition and proportion of solid propellants were determined according to the principle of propellant gas production and oxygen balance, and then the solid-propellant blasting test of simulation coal bodies was carried out. Based on the results and the theory of damage fracture mechanics, the blasting damage fracture process and mechanism of coal from solid-propellant blasting were analyzed. It provides a reference

for the practical application of solid-propellant blasting technology in low-permeability coal seams.

2. Development of Solid Propellant

Solid propellants are mainly composed of a heating agent, gas supply agent, oxygen supply agent, and other components. The oxygen supply agent provides oxygen to the heating agent, causes the oxidation reaction to occur, and releases a lot of heat, and then the gas generating agent is thermally decomposed to produce a large amount of gas. Solid propellants utilized as a coal seam anti-reflection technology should first meet the requirements of gas produced to be non-toxic, harmless, and non-corrosive; secondly, the coal body after solid-propellant blasting does not produce a small crushing zone, and the energy utilization rate is improved as much as possible. Thirdly, the gas production of a solid propellant is large, which can steadily drive the crack to expand within the range. Finally, safety must be ensured during the production process and usage of solid propellants.

A solid propellant is essentially a weak explosive. Therefore, based on the principle of zero oxygen balance of explosives, the authors chose aluminum powder as the heating agent, ammonium perchlorate as the oxygen donor and the main gas generating agent to make a solid propellant. The solid propellant's composition and ratios are shown in Table 1. The main role of HTPB is as an adhesive to bond various materials together, and can give the propellant moisture-proof and antistatic properties. The role of ammonium oxalate is to decompose after heating to produce ammonia to inhibit the decomposition rate of ammonium perchlorate, thereby controlling the gas production rate. The oxygen balance values of three solid propellants with high, medium, and low burning rates were 1.6%, −6.2%, and −18.6%, respectively. The positive oxygen-balance explosives have better detonation performance, but the micro-negative oxygen-balance explosives are safer.

Table 1. Composition and ratio of solid propellant.

Raw Material	Specification	Percentage (%)		
		High Burning Rate	Secondary Burning Rate	Low Burning Rate
HTPB	Type I	13.39	17.37	24.19
TDI	Industrial grade			
KZ	Industrial grade	3.50	4.50	4.23
AP	Type I	0.00	68.00	0.00
AP	Type III	73.00	0.00	61.00
AP	Type IV	5.00	5.00	5.20
Ammonium oxalate	Industrial grade	0.00	0.00	2.50
AL	Industrial grade	5.00	5.00	0.00
Others		0.11	0.13	2.88

Note: (1) HTPB (HO- [CH2CH = CHCH2] n-OH) is hydroxyl-terminated polybutadiene; (2) TDI($C_9H_6N_2O_2$) is toluene diisocyanate; (3) KZ($C_{26}H_{50}O_4$) is dioctyl sebacate; (4) AP(NH_4ClO_4) is ammonium perchlorate; and (5) AL is aluminum.

Under high-temperature conditions, ammonium perchlorate decomposes to produce oxygen, and aluminum powder is oxidized by oxygen to release a lot of heat, which in turn promotes the thermal decomposition of the mixture dominated by ammonium perchlorate to produce a large number of high-temperature and-high pressure gas products. The main reaction equations are shown in Equations (1)–(3).

$$4Al + 3O_2 = 2Al_2O_3 \quad (1)$$

$$2NH_4CLO_4 = N2 + 4H_2O + CL_2 + 2O_2 \quad (2)$$

$$(NH_4)_2C_2O_4 = 2NH_3 + CO + CO_2 + H_2O \quad (3)$$

In order to understand the basic performance parameters of solid propellants, the burning rate, pressure resistance, and temperature resistance of three solid propellants

were tested according to conventional explosives testing methods. The basic performance parameters of the solid propellants are shown in Table 2.

Table 2. Performance parameters of solid propellant.

Name	Recipe Code	*m*/kg	*v*/(mm/s)	V_m(L/kg)	*Q*/(kJ/kg)	ρ/(g/cm^3)	σ/(MPa)	T/(°C/48 h)
Sy-high	YLD	0.3	14	>1400	≥3500	1.4~1.7	120	163
Sy-mid	YLDA	0.3	10	>1200	≥3200	1.4~1.7	120	163
Sy-low	E3	0.3	5	>1091	≥3000	1.4~1.7	120	163

Note: (1) *m* is explosive quantity; (2) *v* is burning rat; (3) V_m is gas production; (4) *Q* is explosion heat; (5) ρ is density; (6) σ is pressure resistance; and (7) T is Temperature resistance.

After a solid propellant is excited, the high-temperature and high-pressure gas is produced in the hole and rapidly expands and impacts the hole wall, thus forming a large range of crack zone around the blast hole, which improves the crack development level of the coal reservoir to a certain extent, dredges the seepage channel, and improves the permeability of coal seam. At the same time, the blasting of a solid propellant will also disturb the dynamic equilibrium state of adsorption and desorption of coalbed methane in the coal reservoir, and finally form disturbance desorption, thermal effect desorption, and replacement desorption of coalbed methane, improving the extraction efficiency of coalbed methane.

3. Experimental Study on Blasting Damage Fracture Process of Coal Solid Propellant

3.1. Test Method

During the field collection and post-processing of the coal samples, secondary disturbance damage occurred inside the coal samples. In addition, the corresponding sensors needed to be placed inside the specimen to obtain the strain waves induced by high-energy gas. This was difficult to achieve in the actual coal samples. Therefore, simulated coal samples were selected as the research sample to carry out the related experimental research work. According to the test results of existing literature [24], the mixing ratio and basic physical and mechanical properties of the simulation coal body are shown in Table 3. Cement, sand, and water were used as the main materials to control the structural strength of the simulated coal body; gypsum, broken coal, perlite, a foaming agent, and mica were used as additional materials to control the micro-cracks, micro-voids, structural planes, and gas of the simulated coal body.

Table 3. Mixing ratio and physical and mechanical properties parameters of simulated coal body.

Materials and Proportioning Sand: Water: Cement: Gypsum: Crushed Mica: Perlite: Foaming Agent	Density ρ (g/cm^3)	Compressive Strength σ_e/MPa	Longitudinal Wave Velocity c_p/(m/s)	Young's Modulus E/GPa
1.4:0.6:1.4:0.2:0.028:0.027:0.048	1.71	12.23	1660	2.32

Note: (1) ρ is density, (2) σ_e is compressive strength, (3) c_p is longitudinal wave velocity, and (4) E is Young's modulus.

Three simulated coal test blocks were made to carry out the blasting test of solid propellants with a high burning rate. The size of the test block was 1000 × 1000 × 600 mm, as shown in Figure 1a. The block was made using manual stirring, tamping, and forming with a small vibrating rod in the template, and manually cured for 28 days. A charge hole with a diameter of 50 mm and a depth of 400 mm was reserved in the middle of the test block. After the solid propellant was placed, it was filled with planting glue and detonated by the ignition powder head. The solid propellant samples and ignition powder head are shown in Figure 1b,c.

(**a**) Simulated coal test blocks (**b**) Propellant charge reel (**c**) Excitation device

Figure 1. The test block and cartridge of solid propellant blasting.

To explore the load characteristics and pressure distribution law in the borehole well from propellant blasting, a pressure sensor and signal acquisition system were used to test the borehole wall pressure. The pressure sensor used was a PVDF piezoelectric film sensor; the pressure signals were collected by the DH5922 N dynamic strain gauge with a sampling frequency of 200 kHz. The test instrument and pressure sensor were arranged as shown in Figure 2.

(**a**) DH5922N dynamic strain meter (**b**) PVDF pressure sensor (**c**) Point diagram

Figure 2. The instruments and measuring point arrangement of hole wall pressure testing.

To explore the degree of damage to coal from solid propellant blasting, the ZT-801 non-metallic ultrasonic detector (Figure a) was used to test the ultrasonic wave velocity before and after blasting. The measuring points were arranged on the horizontal line passing through the center of the charge, the first measurement point was 50 mm from the borehole and each subsequent measuring point was arranged at an interval of 100 mm, as shown in Figure 3. The damage value was calculated with the formula [25] $D = 1 - (v/v_0)^2$ (v_0 and v are the ultrasonic velocities of the test block before and after blasting, respectively).

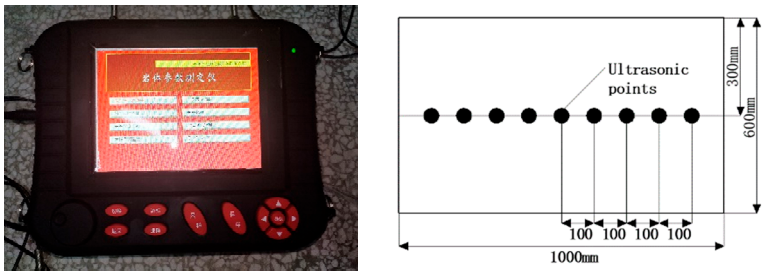

(**a**) (**b**)

Figure 3. Ultrasonic test: (**a**) ZT-801 inorganic non-metallic ultrasonic detector and (**b**) ultrasonic measurement point schematic diagram.

In order to explore the propagation and attenuation law of solid-propellant blasting stress wave in coal, the stress wave was collected by embedding strain bricks in the test block. The strain bricks were embedded in the four positions of 100, 200, 300, and 400 mm

from the center height of the cartridge to the center of the reserved hole. The size of the strain brick was 20 mm × 20 mm × 20 mm, and the proportion of the strain brick was consistent with the large test block. The strain gauge on the strain brick was a BF120-3AA strain gauge. The DH5922N dynamic signal acquisition system was used to collect the strain waveform.

In order to test the crack propagation velocity of coal during the blasting process of the solid propellants, an enameled copper wire with a diameter of 0.14 mm was embedded as a metal probe sensor at a distance of 100 mm between the center of the cartridge and from 50 mm the edge of the blast hole, and the enameled wire was fixed with a U-shaped iron wire. The BSW-3A intelligent five-stage detonation velocity meter was used to test the crack propagation speed in the test block.

The position of the stress wave and crack propagation velocity test sensor is shown in Figure 4.

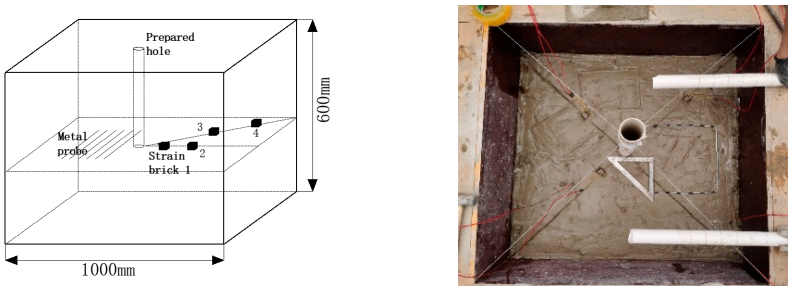

Figure 4. Arrangement of strain brick and metal probes.

3.2. Results and Analysis of Load on Solid-Propellant Blasting Hole Wall

A penetrating crack was formed in all three test blocks after blasting. A half-hole mark of the blast hole was complete, and no crushing zone appeared. The test block after blasting is shown in Figure 5. The representative history curves of the impact pressure time for the middle and bottom hole walls of the blast hole are shown in Figure 6.

Figure 5. The test block after blasting.

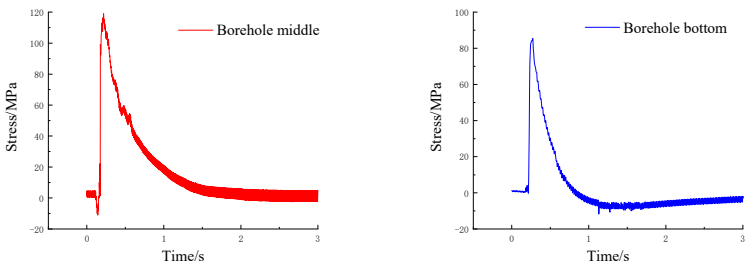

Figure 6. The pressure time history curve of blast hole walls.

It can be seen from Figure 6 that the hole wall pressure after solid-propellant blasting exhibited three stages: transient accumulation pressurization, rapid pressurization, and nonlinear depressurization. The pressure distribution along the whole length of the hole

was uneven, the peak pressure was relatively small, and the pressure action time was relatively long.

After a solid propellant is excited, it decomposes and produces a large number of high-temperature and high-pressure gas products. After a short period of accumulation (0.15 s in the middle of the borehole, and 0.21 s at the bottom of the borehole), the gas products rapidly expanded, impacted the hole wall, and generated a stress wave in the test block, and the hole wall pressure rapidly increased. With the propagation of a stress wave, cracks began to appear in the specimen, high-temperature and high-pressure gas quickly wedged into the crack, and the hole pressure began to nonlinearly decline.

The high-temperature and high-pressure gas products produced by the excited solid-propellant impacted the hole wall and induced the stress wave in the coal near the borehole after a short period of accumulation. When the stress wave intensity was higher than the dynamic compressive (tensile) strength of the coal, the initial crack appears near the borehole, and then the high-temperature and high-pressure gas products began to wedge into the initial crack and drove the crack propagation. Because the ignition end of the solid propellant sample in this test was at the upper part, the initial crack appeared at the upper part of the borehole. When the gas flowed from the upper part of the borehole to the bottom of the borehole, some of the gas leaked from the initial crack in the upper part of the borehole, which caused the peak pressure on the borehole wall to gradually decrease from the upper part of the borehole to the bottom of the borehole. This was consistent with the test results, the peak pressure in the hole (118.1 MPa) was greater than the bottom of the hole (85.4 MPa).

The detonation pressure of an explosion was generally 10~40 GPa, and the detonation velocity of an explosive was generally 1000~8500 m/s [26], so the pressure in the hole was basically uniform in distribution and the loading time was very short. However, the reaction rate of the solid propellants was slow (Table 2) and the impact action was small. The chemical reaction process of the solid propellants was parallel to the impact cracking process of the high-pressure gas product generated by the previous reaction, that is, the formation and diffusion of the high-pressure gas product were also simultaneously carried out. As a result, the pressure in the hole after being blasted with the fracturing agent was relatively small and the pressure maintenance time in the hole was relatively long.

3.3. Results and Analysis of Solid-Propellant Blasting Damage Fracture

The test results of peak strain, damage value, and crack propagation velocity of the coal body from solid-propellant blasting and explosive blasting are shown in Table 4. Among them, the results of coal damage fracture tests from explosive blasting refer to the references [27,28], and the solid-propellant blasting damage fracture results are the average of the valid values of the three test block results.

Table 4. Results of Coal body damage and fracture test.

Results \ Grouping and Points	Grouping	1	2	3	4	5
Peak strain	Solid-propellant blasting	4845	2088	1005	560	
	Explosive blasting	8946	3691	1834	875	
Damage value	Solid-propellant blasting	0.655	0.430	0.304	0.263	0.221
	Explosive blasting	0.865	0551	0.275	0.216	0.161
Crack propagation velocity	Solid-propellant blasting	280.8	162.4	137.4	120.6	109.2
	Explosive blasting	559.5	264.8	187.4	132.6	97.5

According to the table data, the variation curves of stress peak strain, damage, and crack propagation velocity of coal solid-propellant blasting, along with the distance from the center of the blast hole are shown in Figure 7. From Figure 7a, it can be seen that the stress wave intensity in the coal body from propellant blasting is lower, but the decay rate is slower than that of explosive blasting; from Figure 7b, it can be seen that in the adjacent area, the damage value of coal from solid-propellant blasting is less than that of explosive blasting, but with the increase of distance, the damage value of coal from

propellant blasting gradually approaches or even exceeds that of explosive blasting; from Figure 7c, it can be seen that the cracking rate of the coal from propellant blasting is much smaller than that of explosive blasting in the adjacent area, but the two are gradually approaching parity with the increase of distance.

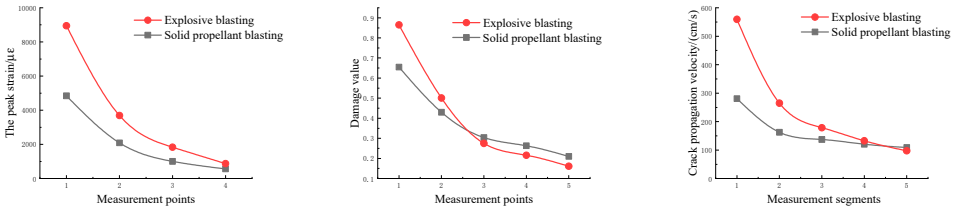

(**a**)Peak strain (**b**) Damage value (**c**) Crack propagation velocity

Figure 7. Peak strain, damage value, and crack propagation velocity of coal body from blasting.

In order to further analyze the process and law of blasting damage and fracturing of coal, the damage test results were expanded by 1000 times, the strain peak was reduced by 10 times, and the crack propagation speed was in the same order of magnitude. The curves of damage, strain peak, and crack propagation speed with distance from the center of the blast hole from propellant blasting and explosive blasting are shown in Figure 8.

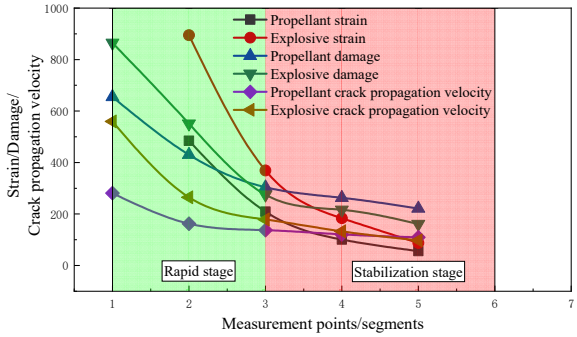

Figure 8. The damage and fracture process curves of coal.

According to Figures 7 and 8, the damage fracture process of the coal body from solid-propellant blasting can be divided into two stages: rapid-damage fracture and slow steady-state damage fracture.

The stress waves generated near the borehole wall by solid-propellant blasting were of low intensity, so no crush zone was generated near the borehole. However, the tensile waves derived from the compressive stress waves can contribute to the initial radial cracking of the coal body that is:

$$\sigma_\theta > (1 - D_0)\sigma_{d\text{tension}}, \sigma_\theta = \sigma_r \cdot \mu / 1 - \mu \quad (4)$$

where σ_θ is the tangential stress generated by the propagation of explosive stress wave in coal, MPa; and μ is Poisson's ratio of coal.

The initial radial crack propagation velocity of coal from solid-propellant blasting was only 280.8 m/s, and the stress wave in the coal caused by propellant blasting rapidly decayed in the adjacent area with the increase of distance, so the crack expansion velocity in the adjacent area of the shell hole, although fast, could expand in a small area. As the distance increased, the attenuated stress wave was unable to continue driving the initial crack propagation in the coal body, as a result, the quasi-static effect of the high-temperature and high-pressure gas products became the main contributor to driving the continued crack propagation. High-temperature and high-pressure gas products wedged into the initial radial crack and drove the crack steady-state expansion from the combined effects of high-temperature and high-pressure gas internal pressure, gas, and original rock stress [29].

Cracks then started to steadily expand when the stress intensity value generated at the crack tip was greater than the fracture toughness of the coal body, that is:

$$2\sqrt{\frac{C}{\pi}}\int_0^a \frac{p(r)}{\sqrt{a^2-r^2}}dr - \sigma_\infty\sqrt{\pi C} \geq K_{IC} \tag{5}$$

where a is the initial radial crack length, m; σ_∞ is the original rock stress, MPa; K_{IC} is the dynamic fracture toughness of coal; $p(r)$ is the gas pressure on the crack surface, MPa; and $P(r) = P_0 \cdot (a-r)/a$, where P_0 is the initial impact compressive stress on the hole wall, MPa.

As the crack continues to expand, the gas pressure in the crack decreases, but the free gas desorbed is involved in driving the further expansion of the crack for the pressure reduction in the crack and the dynamic disturbance of the solid-propellant blasting. At the same time, under the quasi-static stress field of high-pressure gas products and gas, the brittleness of coal increases with the increase of gas pressure. Therefore, when the tangential stress at the crack tip is greater than the critical stress of crack propagation, the crack continues to slowly propagate in a steady state.

$$\frac{a}{r^2}\left[r_0 p_0 + \int_{r_0}^a p(r)dr + \int_{r_0}^a p'(r)dr\right] - \sigma_\infty\left(1+\frac{a^2}{r^2}\right) \geq \sqrt{\pi/4a}K_{IC} \tag{6}$$

where r_0 is the radius of the blast hole, m; $p'(r)$ is the gas pressure at the crack surface, MPa; and because the gas pressure is smaller than the detonation gas pressure, the gas pressure in the crack is usually taken as a constant, namely $p'(r) = p_g$ (p_g is the gas pressure in coal).

At the same time, solid-propellant blasting is a sustainable and slow reaction. The solid propellant that reacts in the middle and late stages of the crack-formation process of the high-pressure gas product produced by the earlier reaction will continue to produce high-temperature and high-pressure gas products. Therefore, the high-pressure gas that drives crack propagation will not decrease too quickly, and is similar to the uniform internal pressure that drives crack propagation. This is the main reason for the steady-state slow propagation process of crack formation in coal from solid-propellant blasting. Moreover, it can be observed from Formula (6) that with the slow propagation of crack length, the critical stress required for the continuous propagation of brittle fracture cracks in coal will continue to decrease, and the lower tangential stress can drive the crack to continue to slowly propagate. Therefore, the crack propagation range is large, although the crack propagation speed in this stage is only 109.2~137.4 m/s.

4. Conclusions

(1) The impact pressure of the hole wall for solid-propellant blasting exhibits three stages: temporary accumulation pressurization, rapid pressurization, and nonlinear depressurization. The pressure is unevenly distributed, and the peak pressure is smaller than that of explosive blasting, but the time of pressure exertion is relatively long, which is more conducive to improving its energy utilization.

(2) The crack propagation velocity and stress wave intensity of coal are small from propellant blasting, but the crack propagation velocity and stress wave slowly attenuate with the increase of distance, which can cause a wide range of crack area and effectively improve the permeability of the coal reservoir.

(3) The damage and cracking of coal from propellant blasting is due to the combined effect of blast stress waves, high temperature and pressure gases, gas, and original rock stress. The damage fracture process can be divided into two stages: the rapid development stage dominated by stress wave action and the slow development stage dominated by the quasi-static action of gas products.

Author Contributions: Conceptualization, H.C. and M.Y.; methodology, H.C. and G.Z.; software, B.S.; validation, H.W.; formal analysis, H.C.; investigation, M.Y.; resources, H.C.; data curation,

D.W.; writing-original draft preparation, H.C.; writing-review and editing, M.Y.; visualization, S.Y.; supervision, D.W.; project administration, J.X. All authors have read and agreed to the published version of the manuscript.

Funding: This research was funded by the National Natural Science Foundation of China (No. 51874123, 11542019), and the Henan Research Program of Foundation and Advanced Technology (No. 162300410032).

Data Availability Statement: The data in this manuscript have been presented in Tables 1–4.

Acknowledgments: The authors thank Siyuan Zhu, Zhen Chen, and Zhiqiang Ren for their guidance on the experiment in this paper. The authors also thank the anonymous reviewers for their remarks which improved the paper.

Conflicts of Interest: The authors declare no conflict of interest. The authors declare that they have no known competing financial interests or personal relationships that could appear to have influenced the work reported in this paper.

References

1. Zou, Q.M. Under The Dual Carbon Target, Coal Should Not Only Practice Decarbonization Transformation, but Also Pay Attention to the Bottom Guarantee. Available online: http://nyj.guizhou.gov.cn (accessed on 31 May 2021). (In Chinese)
2. Wang, X.L. In Proceedings of the Speech at the Opening Ceremony of the 2016 National Coal Fai, Taiyuan, China, 19–20 July 2016. Available online: https://www.meitanwang.com/meitan/b1/851876.html (accessed on 31 May 2021). (In Chinese).
3. Yuan, L. Study on development and utilization strategy of Coalbed methane in China. In Proceedings of the Chinese Academy of Engineering Major Consulting Project Research Achievements, Beijing, China, 29 July 2013. (In Chinese).
4. Hu, J.; Feng, K.W.; Sun, C.; Chen, Y. Research on pressure-relief gas drainage mode of adjacent coal seams in upper protective layer mining of close thin coal seam group. *J. Saf. Sci. Technol.* **2021**, *11*, 65–71. (In Chinese)
5. Liu, S.; Yang, K.; Zhang, T. Rib spalling 3D model for soft coal seam faces with large mining height in protective seam mining: Theoretical and numerical analyses. *Geofluids* **2020**, *2020*. [CrossRef]
6. Zhao, X.; Huang, B.; Wang, Z. Experimental Investigation on the Basic Law of Directional Hydraulic Fracturing Controlled by Dense Linear Multi-Hole Drilling. *Rock Mech. Rock Eng.* **2018**, *51*, 1739–1754. [CrossRef]
7. Hu, S.Y.; Guan, S.W.; Feng, G.R.; Han, D.D.; Chen, Y.B. Effect of hydraulic fracture closure on the void ratio of proppant particles in coalbed methane reservoir. *J. Nat. Gas Sci. Eng.* **2020**, *75*, 103111. [CrossRef]
8. Gao, S.H.; Wang, M.Y. Study on hydraulic fracturing-deep hole pre-splitting blasting composite permeability enhancement technology. *Coal Sci. Technol.* **2018**, *48*, 1–8.
9. Zheng, P.; Xia, Y.; Yao, T.; Jiang, X.; Xiao, P.; He, Z. Formation mechanisms of hydraulic fracture network based on fracture interaction. *Energy* **2022**, *243*, 123057. [CrossRef]
10. Jew, A.D.; Druhan, J.L.; Ihme, M.; Kovscek, A.R.; Battiato, I.; Kaszuba, J.P.; Bargar, J.R.; Brown, G.E., Jr. Chemical and Reactive Transport Processes Associated with Hydraulic Fracturing of Unconventional Oil/Gas Shales. *Chem. Rev.* **2022**, *122*, 9198–9263. [CrossRef]
11. Du, J.; Liu, J.; Zhao, L.; Liu, P.; Chen, X.; Wang, Q.; Yu, M. Water-soluble polymers for high-temperature resistant hydraulic fracturing: A review. *J. Nat. Gas Sci. Eng.* **2022**, 104673. [CrossRef]
12. Li, P.; Zhang, X.; Li, H. Technology of coupled permeability enhancement of hydraulic punching and deep-hole pre-splitting blasting in a "three-soft" coal seam. *Mater. Technol.* **2021**, *55*, 89–96.
13. Xia, J.; Dou, B.; Tian, H.; Zheng, J.; Cui, G.; Kashif, M. Research on initiation of carbon dioxide fracturing pipe using the liquid carbon dioxide phase-transition blasting technology. *Energies* **2021**, *14*, 521. [CrossRef]
14. Yan, S.Y.; Yang, X.L.; Chu, H.B.; Wang, C. Experimental Study on the Dynamic Response and Pore Structure Evolution of Coal under High-Pressure Air Blasting. *ACS Omega* **2022**, *7*, 24475–24484. [CrossRef]
15. Zhang, Y.M.; Meng, Z.Z.; Qin, Y.; Zhang, Z.F.; Zhao, Y.Z.; Qiu, A.C. Innovative engineering practice of soft coal seam permeability enhancement by controllable shock wave for mine gas extraction: A case of Zhongjing Mine, Shuicheng, Guizhou Province, China. *J. China Coal Soc.* **2019**, *44*, 2388–2400. (In Chinese)
16. Lin, B.Q.; Wang, Y.H.; Yan, F.Z.; Zhang, X.L.; Yang, W.; Zhu, C.J. Experimental study of the effect of NaCl solution on the pore structure of coal body with high-voltage electrical pulse treatments. *J. China Coal Soc.* **2018**, *43*, 1328–1334. (In Chinese)
17. Jiang, Y.D.; Xian, X.F.; Liu, Z.F. Experiment and mechanism for enhancing coalbed penetrating coefficient with ultrasonic vibration. *J. Liaoning Tech. Univ.* **2009**, *28*, 236–239. (In Chinese)
18. Shi, Q.M.; Qin, Y.; Li, J.Q.; Wang, Z.W.; Zhang, M.J.; Song, X.J. Simulation of the crack development in coal without confining stress under ultrasonic wave treatment. *Fuel* **2017**, *205*, 222–231. [CrossRef]
19. Qin, L.; Zhai, C.; Liu, S.; Xu, J. Factors controlling the mechanical properties degradation and permeability of coal subjected to liquid nitrogen freeze-thaw. *Sci. Rep.* **2017**, *7*, 3675. [CrossRef] [PubMed]
20. Ao, W.; Fan, Z.; Liu, L.; An, Y.X.; Ren, J.R.; Zhao, M.T.; Liu, P.J.; Li, L.K.B. Agglomeration and combustion characteristics of solid composite propellants containing aluminum-based alloys. *Combust. Flame* **2020**, *220*, 288–297. [CrossRef]

21. Zhang, T.; Zhang, X.; Li, N.; Li, K. High-energy perforation and fracturing (HEPF): Great Revolution of Perforation for 21st Century. In Proceedings of the International Oil and Gas Conference and Exhibition in China, Beijing, China, November 2000. [CrossRef]
22. Jaimes, M.G.; Castillo, R.D.; Mendoza, S.A. High energy gas fracturing: A technique of hydraulic pre-fracturing to reduce the pressure losses by friction in the near wellbore: A Colombian field application. In Proceedings of the SPE Latin America and Caribbean Petroleum Engineering Conference, Mexico City, Mexico, 16–18 April 2012.
23. Li, J.; Cao, L.; Guo, B.; Zhang, X. Prediction of productivity of high energy gas-fractured oil wells. *J. Pet. Sci. Eng.* **2018**, *160*, 510–518 [CrossRef]
24. Chu, H.B.; Yang, X.L.; Yu, Y.Q.; Liang, W.M. Experimental research of the choice for coal blasting simulation material. *Coal Sci. Technol.* **2010**, *8*, 31–33. (In Chinese)
25. Zhao, B.; Wang, H. Different technologies of permeability enhancement of single coal seam in china and new technique of high pressure gas shock. *Blasting* **2014**, *31*, 32–41. (In Chinese)
26. Luo, L.M.; Xie, J.P. Effects of detonation velocity on medium deep hole blasting. *Copp. Eng.* **2021**, *1*, 27–30. (In Chinese)
27. Chu, H.B.; Yang, X.L.; Liang, W.M.; Yu, Y.Q. Study on the damage-fracture process and mechanism of coal blasting. *J. Min. Saf. Eng.* **2018**, *35*, 410–414. (In Chinese)
28. Chu, H.B.; Wang, J.X.; Yang, X.L.; Liang, W.M. Action mechanism of methane gas in the process of coal blasting damage and fracture. *J. Min. Saf. Eng.* **2014**, *31*, 494–498. (In Chinese)
29. Yang, X.L.; Wang, S.R. Meso-Mechanism of damage and fracture on rock blasting. *Explos. Shock. Waves* **2000**, *20*, 247252. (In Chinese)